Journal of Power Sources 206 (2012) 29–36

Contents lists available at SciVerse ScienceDirect

Journal of Power Sources

journal homepage: www.elsevier.com/locate/jpowsour

Combinatorial screening for methanol oxidation catalysts in alloys of Pt, Cr, Co and V

Yuan Zhang*, Paul J. McGinn

Department of Chemical and Biomolecular Engineering, University of Notre Dame, Notre Dame, IN 46556, USA

ARTICLE INFO

Article history:
Received 3 October 2011
Received in revised form 5 December 2011
Accepted 1 January 2012
Available online 31 January 2012

Keywords:
Methanol electro-oxidation
Direct methanol fuel cell
Combinatorial synthesis
High-throughput screening

ABSTRACT

Thin film combinatorial sputter-deposited ternary Pt–Cr–V, Pt–Co–Cr, and quaternary Pt–Co–Cr–V catalysts for methanol electro-oxidation in direct methanol fuel cell were studied. Several compositions exhibited better MOR activities than pure Pt based on the peak current density and onset potential of the methanol oxidation reaction measured by voltammetry. Alloying 43% vanadium with pure platinum gave higher electrocatalytic activity evidenced by 5.9 times greater peak current density. $Pt_{30}Co_{40}Cr_{30}$ outperformed pure Pt by 12× in a ternary Pt–Co–Cr library. Alloying of vanadium into optimum PtCoCr compositions further improved methanoloxidation kinetics. $Pt_{25}Co_{25}Cr_{25}V_{25}$ showed the highest catalytic activity with a peak methanol oxidation current density that was 17× higher than pure Pt and 1.5× higher than $Pt_{33}Co_{33}Cr_{33}$. Atomic absorption studies of dissolved species in the electrolyte showed Co and Cr dissolution at higher rates than V, showing that the chemical ratio of Cr:Co:V in $Pt_{25}Co_{25}Cr_{25}V_{25}$ changed to 0.738:0.862:1.000 after voltammetry. XPS analysis of $Pt_{25}Co_{25}Cr_{25}V_{25}$ revealed a Pt-rich PtV binary compositional surface (Pt:V = 89.04%:10.96%) formed after electrochemical testing. The active catalytic performance and good stabilities of catalysts in the PtCoCrV system suggest them as promising alternatives to Pt–Ru for methanol oxidation.

1. Introduction

Methanol electro-oxidation reaction (MOR) catalysts have attracted much interest over the last decade for applications in direct methanol fuel cells (DMFC). The use of methanol as liquid fuel provides easy handling and re-fueling compared with other types of fuel cells. DMFCs provide great promise to meet increasing power demands from portable electronics devices and to become a good alternative to lithium ion batteries. However, the CO poisoning is commonly observed on the anodes of DMFCs and causes the low catalytic activities of such anodes [1].

The use of PtRu alloy catalysts [2–5] has greatly improved CO tolerance. Further modification of PtRu catalysts by alloying with transition metals achieved higher MOR performance and reduced costs for Pt and Ru [6,7]. A variety of ternary and quaternary Pt–Ru based catalysts have been reported as promising catalysts, such as PtRuNi [8,9], PtRuCo [10–12], PtRuW [13,14], PtRuOsIr [15], PtRuIrSn [16], PtRuCoW [17], and PtRuMoW [18]. However, Ru dissolution at the anode was observed in long term operation [19–22]. Dissolved Ru crosses through the membrane over to the cathode and lowers the overall performance of DMFCs. Therefore, a stable, Ru-free, high MOR activity and low cost anode catalyst is desirable.

Most research on Ru free MOR catalysts has involved alloying Pt with Pd [23,24], Co [25–27], Ni [28–30], and Ti [31,32]. However, the investigated systems have primarily been limited to binary and a few ternary compositions since it is time-consuming and expensive to discover a wide range of ternary and more compositional alloys by conventional process techniques. Combinatorial methods involve parallel synthesis and high-throughput analysis of a large number of samples in a reduced time. Since Reddington et al. [15] reported the first combinatorial study on electrocatalysts using an inkjet printer and fluorescent acid–base indicators, a variety of high-throughput screening methods have been applied to search for better electrocatalysts [33–40]. We reported a thin film combinatorial method employing physical vapor deposition (sputtering) along with a multielectrode half cell system which achieved quantitative, rapid parallel screening of thin film combinatorial libraries [41,42]. Using this thin film approach many binary and ternary combinations of Pt, Ru, Co, W, Ni, Cr, and Cu were examined for improved electrocatalysis. Recently, the optimum compositions obtained from the combinatorial screening of thin film PtNiCr, PtRuCu and PtCoCr libraries were verified by synthesizing a powder versions [29,30,43], which exhibited better performance than a comparable PtRu powder on a noble metal mass basis.

* Corresponding author at: 182, Fitzpatrick Hall, University of Notre Dame, Notre Dame, IN 46556-5637, USA. Tel.: +1 574 631 5692; fax: +1 574 631 8366.
E-mail address: yzhang8@nd.edu (Y. Zhang).

0378-7753/$ – see front matter © 2012 Elsevier B.V. All rights reserved.
doi:10.1016/j.jpowsour.2012.01.016

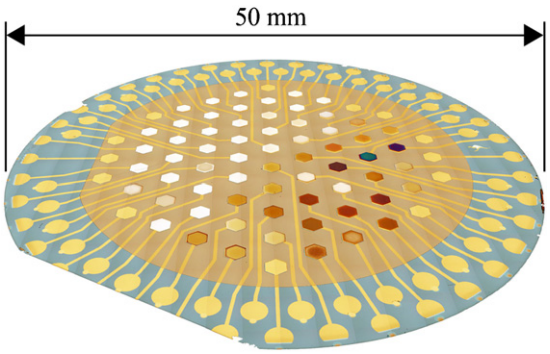

Fig. 1. Composite micrograph image of a Pt–Co–Cr combinatorial library on a 50 mm Si wafer.

In the present work, we investigate vanadium additions as a means to further enhance MOR catalytic activities. Additions of vanadium may favor the formation of oxygenated species and oxidize absorbed CO on Pt surface at a lower potential. Several compositions with excellent methanol oxidation activities were identified in ternary Pt–Cr–V and Pt–Co–Cr systems. Furthermore, we introduced vanadium as fourth metal, alloying with ternary Pt–Co–Cr to examine the performance of more complex quaternary alloys.

2. Experimental procedures

The preparation of the thin film combinatorial composition libraries and the subsequent electrochemical testing has been described in detail previously [41,42]. Briefly, combinations of high purity Pt, Co, Cr and V were sputter deposited through shadow masks to yield an array of discrete multilayer spots on 2 inch diameter silicon wafers. The samples were vacuum annealed at 550 °C for 4 h followed by a rapid insertion high temperature anneal at 900 °C for 5 min in a separate furnace after deposition to transform the multilayer samples into homogenous alloys.

An example of a combinatorial library after annealing is shown in Fig. 1. The hexagonal pads across the center of the wafer are the library members, while circular probe contacts are positioned around the perimeter of the wafer. A matching circular array of spring-loaded probes provides the connection between a multichannel potentiostat and the library.

A commercial multielectrode potentiostat system (Scribner Associates Model 900B Multichannel Microelectrode Analyzer (MMA)) is used for electrochemical testing. A specially designed sample cell permits simultaneous collection of cyclic voltammograms from all of the combinatorial library members. The method utilized to screen catalyst compositions for methanol oxidation has been previously described [41]. Briefly, for MOR characterization, extra dry nitrogen was bubbled through the electrolyte (0.5 M H_2SO_4). The potential was swept at 10 mV s^{-1} from −0.3 V to 1.1 V-SCE for 10 cycles so the CV curves stabilized, and were then measured from all the catalyst pads. With the introduction of 0.82 mL methanol (equivalent to 0.5 M in 40 mL solution), the cell was maintained at −0.2 V SCE for 270 s permitting the solution to saturate and the current to stabilize. Following the introduction of the methanol, the potential was again swept from −0.3 to 1.1 V-SCE at 10 mV s^{-1} until reasonably stable curves were again measured from all of the catalyst pads. A conditioning process was applied to each library at various temperatures (25, 40 and 60 °C) as described previously [41]. The behaviors of the various catalyst compositions were compared by using the onset potential where methanol oxidation begins and the peak current density of the reaction. The onset potential was defined at the intercept of the curve with a specific current density of 5×10^{-5} A cm^{-2}. The onset potential was applied since it is not affected by changes of surface roughness and showed a strong correlation with catalytic activity in our previous work [41]. The current density at the peak of the methanol reaction is based on the geometric area of the sample pad (0.026 cm^2) and not the active area. The active area of platinum surfaces is usually determined by examining a monolayer adsorption during a potential sweep. The present combinatorial approach necessitates reporting currents from widely varying compositions, including some with no platinum at all. These compositions have an overpotential for the adsorption of H^+ or other species and their active area cannot be defined in situ by these methods. Other methods to determine roughness, such as Differential Electrochemical Mass Spectroscopy (DEMS) or STM are not compatible with the present combinatorial testing approach.

X-ray diffraction (Bruker D8 discover with an area detector) was used for structural characterization of select thin film libraries before the electrochemical testing. Automated optical microscopy (Olympus BX70 DP70 microscope with a Prior stage and DP70 camera) was applied to photograph each sample on a library before and after electrochemical testing. The method to evaluate surface degradation based on microscopy imaging is described in a previous report [42]. The surface condition of each library was visually assessed and qualitatively scored from 0 to 5 to assess different levels of corrosion. A score of 5 signifies no obvious deterioration, 4 signifies some discoloration, 3 means the pad is spalled, with ragged patches flaking off, 3 means the pad perimeter is shrinking, 1 denotes spalling and shrinking, while 0 denotes disappearance of the pad, with no trace of the catalyst remaining. Finally, duplicate libraries are synthesized and characterized to insure that the experimental results are consistent.

Catalyst chemical modification was quantitatively assessed by measuring metal leaching from selected blanket thin film catalyst compositions as a function of voltammetric cycling at different temperatures. The optimal alloy composition was selected from the combinatorial library and a blanket film was sputtered on a 2 in. blank silicon wafer. The film was vacuum annealed at 550 °C for 4 h then at 900 °C for 5 min to achieve same homogeneous microstructure as in the libraries. The blanket alloy film was conditioned by the standard MOR cycling at 60 °C. Electrolyte samples were collected after the electrochemical testing was completed at 25 °C, 60 °C and 25 °C. Perkin Elmer Atomic Adsorption Spectrometry (AA) was applied to obtain the concentration of ions in the electrolyte solutions and determine the extent of metal leaching in the different test cycles. XPS analysis was performed to investigate the compositional state of the surface of the optimal alloy before and after voltammetric cycling. XPS spectra were taken at room temperature using a Kratos XSAM800 X-ray Photoelectron Spectrometer. Data was acquired using a Mg k-alpha X-ray source, and the acquisition software was Kratos Vision 2. All binding energies were calibrated by referencing C 1s (284.50 eV). Data was analyzed using CasaXPS software with the Kratos element library.

3. Results and discussion

3.1. Pt–Cr–V

The results for the Pt–Cr–V library are summarized in Fig. 2. The peak current densities of the MOR are mapped onto a ternary plot. The initial room temperature testing showed weak responses from most of compositions that is characteristic of an unconditioned catalyst surface. Pt rich alloys produced slightly larger current density towards methanol oxidation than other compositional catalysts. Pure Pt was the best performing composition with a current density of 2.35×10^{-4} A cm^{-2} (Fig. 2a). Following conditioning at 60 °C the

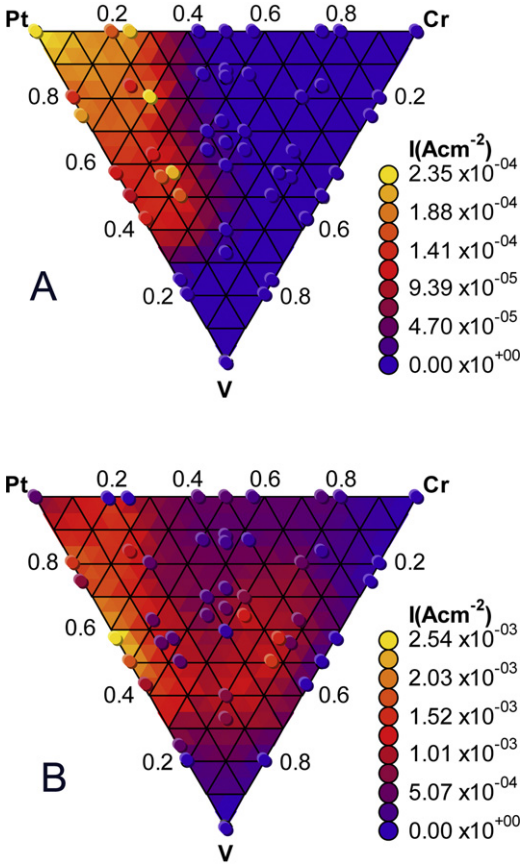

Fig. 2. (a) Peak current densities and (b) onset potentials of methanol oxidation for the Pt–Cr–V system. Measurements were taken during the 10th forward scan at 10 mV s^{-1} in 0.5 M H_2SO_4, 0.5 M methanol at 20 °C.

highest activity was shown by binary Pt–V compositions. $Pt_{57}V_{43}$ exhibited the highest peak current of 2.547×10^{-3} A cm^{-2} (Fig. 2b) and the lowest onset potential of 0.23 V-SCE. The improved MOR current density is more than 5 times the value for the conditioned pure Pt catalyst. Pt–Cr–V compositions were imaged by optical microscopy before and after testing. Different levels of corrosion were scored from 0 to 5 and plotted in Fig. 3. Excellent scores were obtained in optimum PtV binary compositions, indicating good durability in these samples. The surface of the optimum catalysts

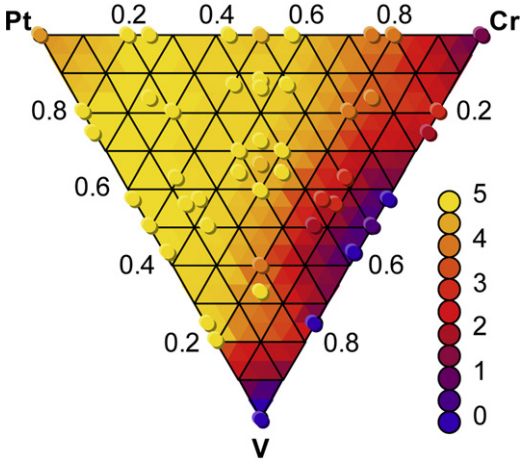

Fig. 3. Visually assessed corrosion scores for the Pt–Cr–V system.

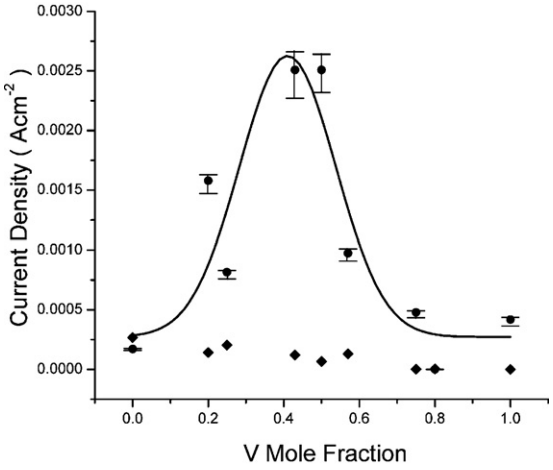

Fig. 4. Peak methanol oxidation current densities of a Pt–V library before (♦) and after conditioning (●). Measurements were taken during the 10th potential sweep in nitrogen saturated 0.5 M H_2SO_4, 0.5 M CH_3OH at 10 mV s^{-1}.

was intact and exhibited no sign of degradation after electrochemical testing.

The testing results of the binary Pt–V compositions in the PtCrV library before and after the conditioning process are shown in Fig. 4. Where there are multiple data points for the same composition the standard deviation was used to define the error bars. The presence of vanadium did not improve the methanol oxidation reaction for room temperature testing of unconditioned samples. However, a noticeable current density improvement with V additions was observed when the library was conditioned. The trend is plotted by a Gaussian fit that identifies the peak MOR performances in $Pt_{57}V_{43}$ and $Pt_{50}V_{50}$.

The improvement of MOR activity by the 60 °C treatment is not fully understood but a recent study [44,45] on PtRu and PtNiCr particle electro-oxidation catalysts suggested the cause is the formation of reversible metal (hydrous) oxides state and with some effect also due to changes in surface area due to metal dissolution. Few studies have examined vanadium in alloyed anode catalysts but several reports suggest vanadium pentoxide (V_2O_5) as a good oxidation catalyst for methanol [46–49]. Maiyalagan found a Pt/V_2O_5–C electrode exhibits higher catalytic MOR activity than Pt/C and also showed comparable stability [50]. The high catalytic activity of vanadium oxide (VO^{2+}/V^{3+}) in a Pt electrode is attributed to a bifunctional mechanism similar to that for well-known Pt–Ru catalysts [51]. Vanadium (hydrous) oxides form a surface oxy-hydroxide which subsequently oxidizes and removes CO_{ad} intermediates at a lower potential by providing a sufficient amount of OH_{ad}. The onset potential of $Pt_{57}V_{43}$, which is 170 mV lower than a conditioned pure Pt catalyst, suggests the contribution of a vanadium oxide/hydrous oxide in the $Pt_{57}V_{43}$ catalyst. The possibility that some activity increase might also be due to increased surface area resulting from transition metal dissolution is suggested by our previous studies on the PtNiCr system [41,44,45]. For example a Pt enriched surface induced by slight leaching of vanadium could also contribute to the significant improvement observed in the optimum binary compositions. This is examined in more detail in the Pt–Co–Cr–V alloys below.

3.2. Pt–Co–Cr

The Pt–Co–Cr system was investigated in an earlier report [42]. This system was revisited as part of the present study since some aspects of the previous testing protocol had been modified. The recent re-examination of Pt–Co–Cr thin film libraries

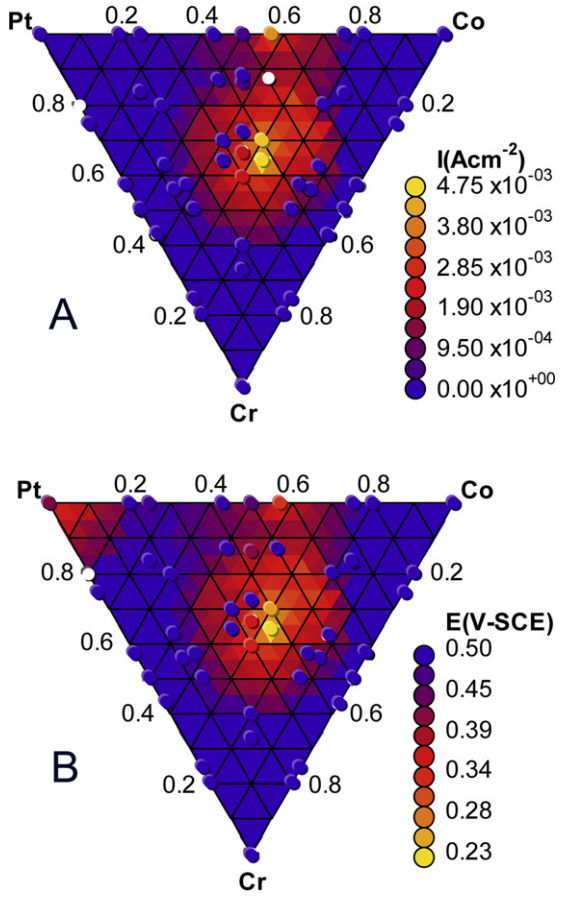

Fig. 5. (a) Peak current densities and (b) onset potentials of methanol oxidation for the Pt–Cr–Co system.

exhibited similar trends to those previously reported. The results for the methanol eletro-oxdiation reaction with a conditioned PtCoCr library are shown in Fig. 5. The samples around $Pt_{33}Co_{33}Cr_{33}$ showed excellent MOR activities. $Pt_{30}Co_{40}Cr_{30}$ had the highest activity and it exceeded the system's current measurement limits. Extrapolation of its cyclic voltammetry curve implies it would have a peak current density of 4.75×10^{-3} A cm^{-2}, which was 12 times the current of the Pt samples. It had an onset potential of 0.23 V-SCE, 200 mV lower than the pure Pt catalyst. A cluster of compositions around $Pt_{33}Co_{33}Cr_{33}$ showed no visual difference before and after testing, suggesting satisfactory corrosion resistance by these compositions. Fig. 5 also shows $Pt_{57}Co_{43}$ outperformed all other PtCo binary compositions after conditioning, which was not revealed in the examination reported in our earlier studies. $Pt_{57}Co_{43}$ achieved a current density comparable to $Pt_{30}Co_{40}Cr_{30}$ and a low onset potential of 0.33 V-SCE. It should be noted that $Pt_{57}Co_{43}$ had a corrosion score of 4, slightly worse than $Pt_{30}Co_{40}Cr_{30}$ with a score of 5, indicating $Pt_{57}Co_{43}$ had a more degraded surface after electrochemistry testing.

$Pt_{50}Co_{50}$ was reported as the optimum MOR catalyst in binary Pt–Co system by several groups [52–54]. The final active $Pt_{57}Co_{43}$ composition in this thin film screening is close to the optimum $Pt_{50}Co_{50}$ in the literature. The activity of Pt–Co compositions can benefit from Co leaching, which leads to a more active and rougher Pt surface, as reported by Antolini [55] and Bonakdarpour [56]. Our recent studies on PtCoCr powder catalysts [27] revealed that the performance improvement in $Pt_{33}Co_{33}Cr_{33}$ due to the conditioning process was the result of some dissolution and oxidation of Co and Cr. The poor activities of Pt–Cr catalysts agrees with the results of Yang et al. [57] who found binary Pt–Cr compositions had a worse methanol oxidation performance than pure Pt. But Cr potentially acts as a stabilizer to improve the corrosion resistance in ternary alloys. With nearly 33 at% Cr in the Pt–Co–Cr sample ($Pt_{33}Co_{33}Cr_{33}$ nominal composition), the alloy showed the advantage of better corrosion resistance than Pt–Co binary alloys and the strongest MOR activity.

As recently reported, a powder $Pt_{30}Co_{30}Cr_{40}$ catalyst was synthesized and outperformed PtRu/C catalysts with 160% higher MOR activity [27]. Anodic conditioning of the powder PtCoCr catalyst led to a dramatic increase of the MOR mass activity (27.8 times). This correlation between the results in thin film and powder forms of the alloys shows that compositions in the Pt–Co–Cr system are promising candidates as a Ru-free anode electrocatalysts.

3.3. Pt–Co–Cr–V

The introduction of vanadium to the PtCoCr alloy was examined to see if further performance improvement could be realized. To seek the optimum catalyst in the Pt–Co–Cr–V system, our combinatorial screening method has been further expanded to the quaternary alloys.

The PtCoCrV library consisted of multilayer alloys with up to 32 total layers and a total thickness of 800 Å. Each library had 61 unique compositions spread across the quaternary composition space. After annealing and MMA testing, all the experimental data were visualized in a 3D 4-component compositional tetrahedron to identify the trends. Data sets from a quaternary combinatorial system were generated by an Excel VBA program, visualized using Voxler.

It should be noted that the recorded value of current density, onset potential cannot be directly compared between ternary and quaternary systems due to the variation in ternary and quaternary approaches (total layers, film thickness, etc.). But the trends of all compositions remain in the quaternary libraries and are consistent with those shown in ternary libraries.

Initial unconditioned tests showed that the optimum Pt–Co–Cr ternary compositions benefited from the addition of vanadium (Fig. 6a). $Pt_{17}Co_{50}Cr_{17}V_{16}$ was the most active composition with the highest MOR peak current density of 1.70×10^{-3} A cm^{-2}. The Co rich quaternary alloys exhibited similar strong activities as in the ternary libraries. After conditioning the $Pt_{17}Co_{50}Cr_{17}V_{16}$ alloy performed very poorly because the sample deteriorated in the electrolyte, receiving a zero score in the corrosion screening (Fig. 7). Fig. 6b shows the peak current densities after the library was conditioned. $Pt_{25}Co_{25}Cr_{25}V_{25}$ outperformed the conditioned Pt and had the best MOR current density which exceeded the measurable limit of the MMA system. Extrapolation of its cyclic voltammetry curve implies it would have a peak current density of 4.25×10^{-3} A cm^{-2}. The neighboring composition $Pt_{20}Co_{27}Cr_{27}V_{26}$ showed the best onset potential of 0.089 V-SCE, 170 mV higher than pure Pt. These two optimum quaternary compositions exhibited promising corrosion resistance with excellent scores in Fig. 7. In the quaternary library, $Pt_{33}Co_{33}Cr_{33}$ showed a MOR current density of 2.78×10^{-3} A cm^{-2}, 10 times higher than pure Pt (2.48×10^{-4} A cm^{-2}) but it did not outperform $Pt_{25}Co_{25}Cr_{25}V_{25}$.

To more clearly illustrate the effect of vanadium in PtCoCr alloys, a triangular slice from the quaternary compositional space is shown in Fig. 8. All 14 compositions shown in the slice contained a fixed 1:1 atomic concentration PtCo and a varying ratio of Cr and V. $(PtCo)_{50}Cr_{50}$ (equal to $Pt_{33}Co_{33}Cr_{33}$) recorded the best ternary MOR activity and responded even more strongly with the addition of vanadium. When the vanadium was added up to 25% atom concentration in the quaternary composition, $(PtCo)_{33}Cr_{33}V_{33}$ (equal to $Pt_{25}Co_{25}Cr_{25}V_{25}$) reached the maximum MOR activity with a 52.9% higher peak current density than $Pt_{33}Co_{33}Cr_{33}$. $Pt_{25}Co_{25}Cr_{25}V_{25}$ also exhibited an onset potential of 0.159 V-SCE which was 95 mV

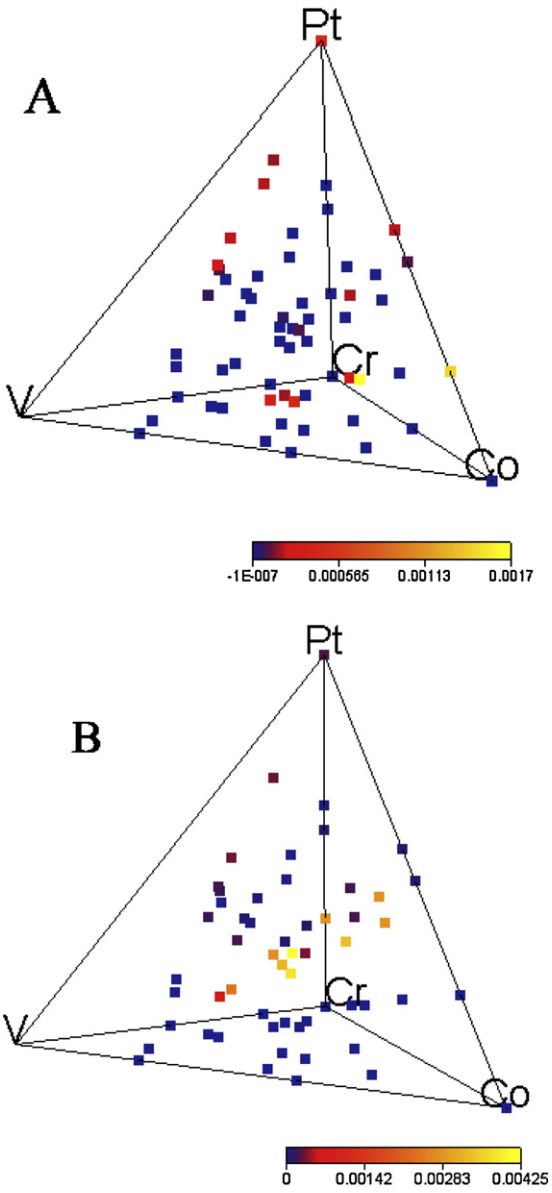

Fig. 6. Peak methanol oxidation current densities for the Pt–Cr–Co–V system (a) before conditioning and (b) after conditioning.

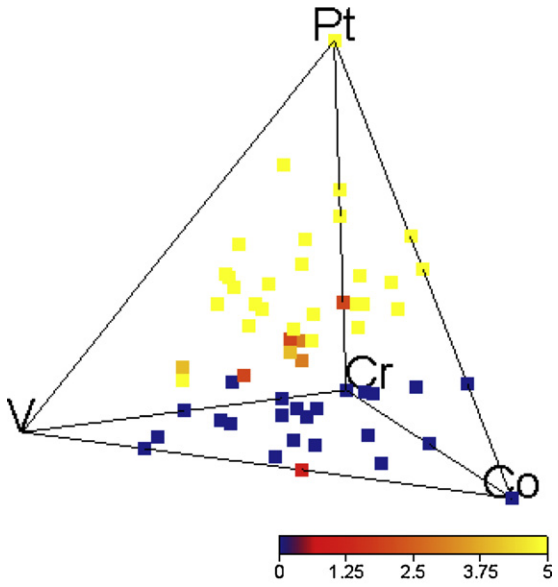

Fig. 7. Visually assessed corrosion scores for the Pt–Co–Cr–V system.

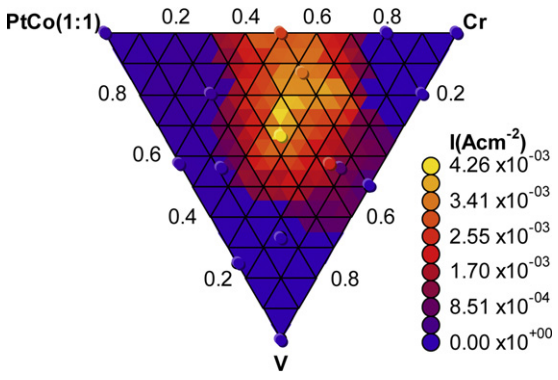

Fig. 8. Peak MOR current density from Pt–Co–Cr–V quaternary screening with fixed Pt:Co (1:1) and varying V and Cr.

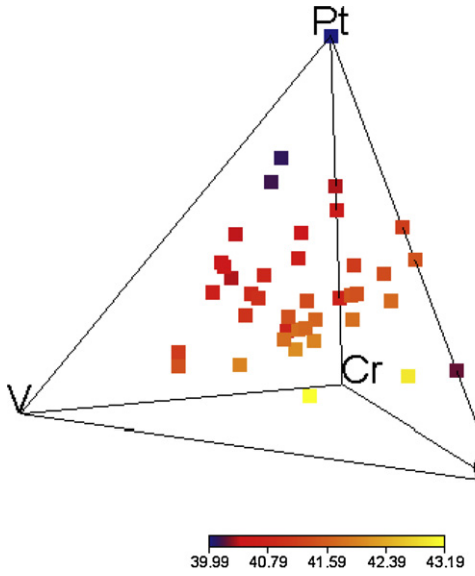

Fig. 9. Quaternary plot of 2Θ shift of the Pt (1 1 1) peak in X-ray diffraction scans of the Pt–Co–Cr–V system.

lower than that of $Pt_{33}Co_{33}Cr_{33}$. The introduction of vanadium may provide the more active sites to oxidize CO to lower the onset potential. Slight leaching of V (see below) may also lead to a Pt enriched surface and hence a higher current density.

The crystallographic structures in the Pt–Co–Cr–V library were characterized by X-ray diffraction after annealing. The Pt (1 1 1) peak was detected in most of the samples. With the addition of other elemental atoms, the Pt (1 1 1) diffraction peak shifts from 39.99° (pure Pt) to a high value of 43.19° ($Pt_{10}Cr_{27}Co_{36}V_{27}$). Fig. 9 shows the extent of 2θ shift across the phase field. The peak shift can be attributed to the incorporation of Cr, Co, V atoms into the Pt lattice, and thus, it reflects the degree of alloying of PtCoCrV compositions. A single phase solid solution of Pt FCC structure was found in the group of compositions around PtCoCrV (1:1:1:1) with the Pt (1 1 1) peaks of these samples shifted to higher angles. These compositions showed excellent MOR activity in electrochemistry testing. The Pt_3Cr phase ((2 0 0) peak) was detected in binary $Pt_{50}Cr_{50}$ and $Pt_{57}Cr_{43}$ alloys, as well as in $Pt_{37}Cr_{50}V_{13}$ and $Pt_{50}Cr_{37}V_{13}$ ternary alloys. All of these compositions performed

Table 1
The amount of dissolved Cr, Co, V in electrolyte samples collected after MOR testing at 25 °C, 60 °C, 25 °C.

Element	Leached amount after initial testing at 25 °C (nmol cm^{-2})	Leached amount after conditioning at 60 °C (nmol cm^{-2})	Leached amount after testing at 25 °C (nmol cm^{-2})	Total leached amount (nmol cm^{-2})	Total leached percentage (%)
Co	1.068	46.783	19.763	67.614	30.71
Cr	2.394	79.687	11.561	93.642	40.71
V	3.045	39.340	6.563	48.948	19.63

poorly towards methanol oxidation. There were no other intermetallic phases detected in the quaternary Pt–Co–Cr–V thin film compositions.

The surface of $Pt_{25}Cr_{25}Co_{25}V_{25}$ after methanol oxidation testing appears unchanged by optical microscopy, but further investigation is needed to determine if there is any surface elemental modification after cycling. A $Pt_{25}Cr_{25}Co_{25}V_{25}$ alloy film was deposited on a 2 in. blank wafer and consisted of 32 total layers with an overall thickness of 800 Å. The electrolyte was analyzed for Co, Cr, and V content to determine the extent of metal dissolution occurring during different test cycles. The moles of leached metal were normalized by the thin film surface area in the reaction and are summarized in Table 1. It should be noted that Pt dissolution could occur from the Pt mesh counter electrode used in electrochemical testing. The amount of Pt leached from the thin film sample is expected to be smaller than that from the counter electrode. Therefore, the Pt content was not monitored in this study. After voltammetric cycling at 25 °C, relatively little Cr, Co, or V was detected. Following conditioning at 60 °C, all of the metals showed a large increase in the extent of dissolution due to the high temperature treatment. Cr dissolution was the greatest with 79.687 nmol cm^{-2} atoms leached from surface. V showed comparatively less dissolution with an amount of 39.340 nmol cm^{-2} detected, still nearly 130 times higher than that in the initial 25 °C testing. The results show that the improvement in activity observed after conditioning was in part due to dissolution of Co, Cr, and V, with the expectation of some modification of the surface composition. It is unclear if substantial surface roughening occurred. With subsequent MOR cycling at 25 °C, Co dissolved to a greater extent than the other metals, with a total of 19.763 nmol cm^{-2} atoms being removed after 20 cycles. The amount of dissolved V was less than Co and Cr, but still almost twice the amount dissolved after initial 25 °C cycling (6.563 nmol cm^{-2} vs. 3.045 nmol cm^{-2}). Based on the total amount of metals leached, it is expected that 59.29% Cr, 69.29% Co and 80.37% V remained in the thin film sample. Hence, after conditioning and cycling, the effective bulk compositional ratio of Cr, Co, V changed from 1:1:1 to 0.738:0.862:1.000. From the CV results, it appears that the higher vanadium content led to more active sites for CO oxidation and a reduced onset potential.

XPS measurements of the $Pt_{25}Cr_{25}Co_{25}V_{25}$ surface before electro-chemical treatment clearly indicated that the surface is mainly composed of Cr and V oxides. Fig. 10a shows the binding energies of the V 2p levels are 524.6 and 516.8 eV, which are very close to those for V_2O_5 bulk samples at room temperature [58]. The chromium 2p peaks were assigned to two groups of different chemical species (Fig. 10b): oxidic or hydroxydic Cr^{III} (Cr_2O_3, $Cr(OH)_3$, 577.0 ± 0.4 eV [59,60]) and Cr^{VI} (CrO_3, 578.3 ± 0.4 eV [61]). Cr_2O_3 was reported to be further oxidized to CrO_3 when the temperature was above 900 °C [62]. Lippitz et al. [63] reported the co-existence of Cr^{III} (Cr_2O_3) and Cr^{VI} (CrO_3) in chromium nitride films after 530 °C annealing in nitrogen atmosphere. In this study, the Cr on the surface was oxidized by the annealing process and formed mixed Cr^{III} and Cr^{VI} oxide phases. Pt $4f_{7/2}$ and $4f_{5/2}$ spectra were observed at 70.8 and 74.2 eV respectively, which are similar to 70.9 and 74.5 eV reported for bulk Pt metal [59]. That indicates Pt was present in the zero-valent state. One small peak was located at 781.10 eV which was assigned to Co(II) oxide phase. The surface compositional ratio (Pt:V:Co:Cr) was calculated to be 3.37%:38.06%:3.72%:44.85% on the basis of the peak areas, as shown in Table 2. The result suggests the surface of $Pt_{25}Cr_{25}Co_{25}V_{25}$ was covered by an oxide skin after the annealing process and only a very small amount of Pt remained in top surface layers. After conditioning and electrochemical testing there was no Cr or Co detected

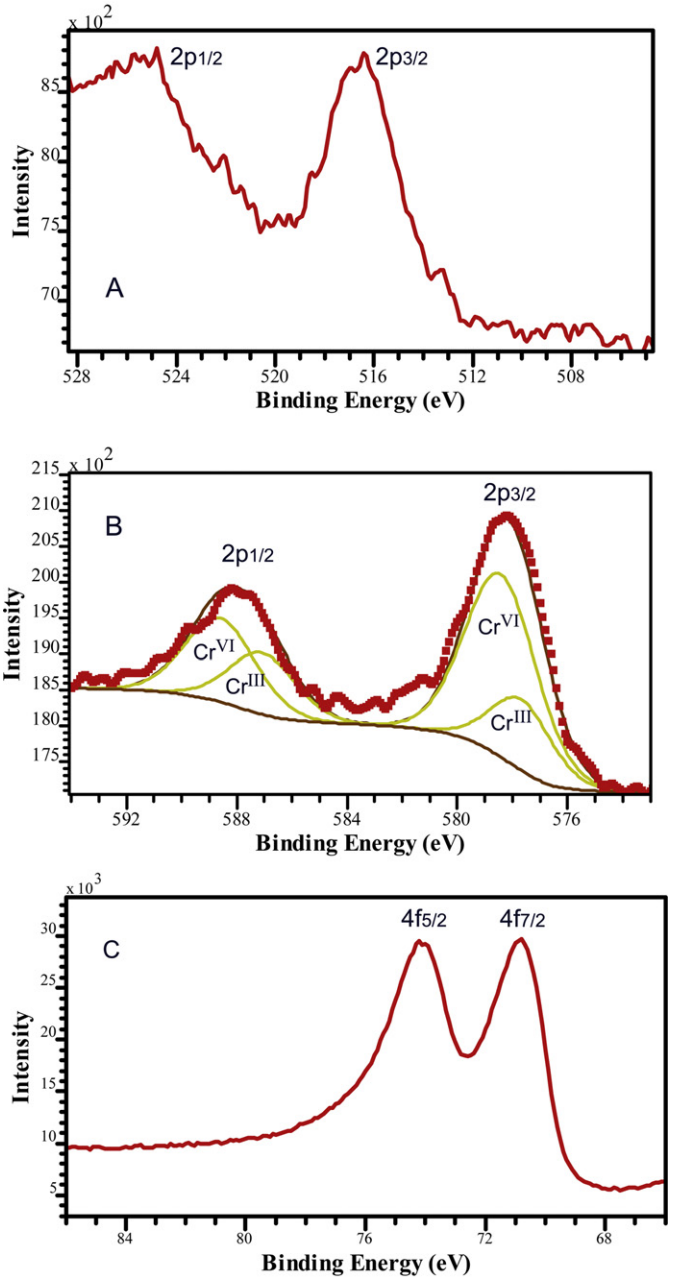

Fig. 10. XPS spectra of $Pt_{25}Cr_{25}Co_{25}V_{25}$ sample (a) V 2p signal before conditioning and cycling, (b) Cr 2p signal before conditioning and cycling and (c) Pt 4f signal after conditioning and cycling.

Table 2
Summary of XPS analysis, atomic % of the elements present for the $Pt_{25}Cr_{25}Co_{25}V_{25}$ in the study.

sample	Pt (atomic %)	Co (atomic %)	Cr (atomic %)	V (atomic %)
Before conditioning	3.37	3.72	44.85	38.06
After conditioning	89.04	0	0	10.96

on the surface. In contrast to the surface before conditioning and cycling, a much higher amount of metallic Pt (70.8 and 74.2 eV) was detected, as shown in Fig. 10c. Small amounts of V 2p were found and can be assigned to V(V) as in V_2O_5. The surface compositional ratio is estimated as Pt:V:Co:Cr = 89.04%:10.96%:0%:0%. The results are given in Table 2. This is in general agreement with the mass ratio dissolved from the surface in the leaching test that indicated more vanadium remained in thin film after cycling relative to Co and Cr. The leaching of transition metal atoms results a severely Pt-enriched surface with small amounts of vanadium oxides present in surface layers.

The leaching of transition metals from catalyst has been observed and studied by several groups [64,65]. Potential cycling has been shown to lead to dissolution of transition metal atoms, resulting in surface roughening [66]. In $Pt_{25}Cr_{25}Co_{25}V_{25}$, the electrochemical Pt surface area is reduced during the annealing process but returns to a significantly increased value by potential cycling. The enriched surface accounts for some of the activity improvement of $Pt_{25}Cr_{25}Co_{25}V_{25}$, but bi-functional effects [2] and an electronic (ligand) effect [67] also are likely contributing causes for the enhanced surface catalytic activities. Vanadium atoms were present within the surface layers and provide more active sites towards CO oxidation, demonstrating the bi-functional mechanism as seen in PtV binary catalysts. Although there were no Co and Cr detected in top surface layer, it is unclear if an optimal compositional CoCrV alloy formed under the surface region that electronically modifies the Pt enriched surface. In the context of combinatorial testing, because compositional neighbors improved to a similar extent, it is likely that such performance improvements ultimately reflect compositional effects more than surface roughness.

4. Conclusions

Pt–Cr–V, Pt–Co–Cr and Pt–Co–Cr–V alloys were examined for MOR catalytic activity by thin film combinatorial synthesis and high-throughput screening. The presence of vanadium in Pt–V alloys was found to significantly improve the methanol oxidation reaction activities. The optimum Pt–V thin film catalyst composition was identified as $Pt_{57}V_{43}$, which showed good durability during electrochemical testing. A cluster of compositions around $Pt_{33}Cr_{33}Co_{33}$ exhibited the highest MOR activity in ternary screening of Pt–Co–Cr alloys.

The screening protocol was extended to quaternary alloys and was used to examine Pt–Co–Cr–V alloys. Further improvement in Pt–Co–Cr MOR activity was observed with the introduction of vanadium. $Pt_{25}Co_{25}Cr_{25}V_{25}$ showed the best MOR activity with 52.9% higher peak current density and 95 mV lower onset potential than $Pt_{33}Co_{33}Cr_{33}$. Testing showed that dissolution of transition metals occurs during conditioning and cycling. Surface examination by XPS indicated a Pt-enriched PtV binary compositional surface formed ($\sim Pt_{89}:V_{11}$) in the PtCoCrV alloy, resulting in strong MOR activity. Based on these results, PtCoCrV catalysts merit further examination for potential use as anode catalysts in direct methanol fuel cells.

Acknowledgments

This work was partially supported by the U.S. Army CECOM RDEC through Agreement DAAB07-03-3-K414 and by the Department of Defense and the Army Research Office through contract numbers W911QX06C0117 and W911NF08C0037. Such support does not constitute endorsement by the U.S. Army of the views expressed in this publication.

References

[1] A.S. Arico, S. Srinivasan, V. Antonucci, Fuel Cells 1 (2001) 133.
[2] M. Watanabe, S. Motoo, J. Electroanal. Chem. 60 (1975) 267.
[3] N.M. Markovic, H.A. Gasteiger, P.N. Ross Jr., Electrochim. Acta 40 (1995) 91.
[4] F.J. Rodriguez-nieto, T.Y. Morante-Catacora, C.R. Cabrera, J. Electroanal. Chem. 571 (2004) 15.
[5] C. Lamy, J.M. Leger, S. Srinivasan, Mod. Aspect. Electrochem. 34 (2001) 53.
[6] E. Antolini, Appl. Catal. B: Environ. 74 (2007) 337.
[7] U.B. Demirci, J. Power Sources 173 (2007) 11.
[8] K.W. Park, J.H. Choi, B.K. Kwon, S.A. Lee, Y.E. Sung, H.Y. Ha, S.A. Hong, H. Kim, A. Wieckowski, J. Phys. Chem. B 106 (2002) 1869.
[9] J. Liu, J. Cao, Q. Huang, X. Li, Z. Zou, H. Yang, J. Power Sources 175 (2008) 159.
[10] P. Strasser, Q. Fan, M. Devenney, W.H. Weinberg, P. Liu, J.K. Norskov, J. Phys. Chem. B 107 (2003) 11013.
[11] X. Zhang, F. Zhang, K.Y. Chan, Catal. Commun. 5 (2004) 749.
[12] P. Strasser, J. Comb. Chem. 10 (2008) 216.
[13] C. He, H.R. Kunz, J.M. Fenton, J. Electrochem. Soc. 144 (1997) 970.
[14] C. Roth, M. Goetz, H. Fuess, J. Appl. Electrochem. 31 (2001) 793.
[15] E. Reddington, A. Sapienza, B. Gurau, R. Vishwanathan, S. Sarangapani, E.S. Smotkin, T.E. Mallouk, Science 280 (1998) 1735.
[16] V. Neburchilov, H. Wang, J. Zhang, Electrochem. Commun. 9 (2007) 1788.
[17] G.S. Chai, J.S. Yu, J. Mater. Chem. 19 (2009) 6842.
[18] W.C. Choi, J.D. Kim, S.I. Woo, Catal. Today 74 (2002) 235.
[19] M.K. Jeon, K.R. Lee, K.S. Oh, D.S. Hong, J.Y. Won, S. Li, S.I. Woo, J. Power Sources 158 (2006) 1344.
[20] M.K. Jeon, J.Y. Won, K.S. Oh, K.R. Lee, S.I. Woo, Electrochim. Acta 53 (2007) 447.
[21] P. Piela, C. Eickes, E. Brosha, F. Garzon, P. Zelenay, J. Electrochem. Soc. 151 (2004) A2053.
[22] Y. Chung, C. Pak, G.S. Park, W.S. Jeon, J.R. Kim, Y. Lee, H. Chang, D. Seung, J. Phys. Chem. C 112 (2008) 313.
[23] S. Papadimitriou, A. Tegou, E. Pavildou, G. Kokkinidis, S. Sotiropoulos, Electrochim. Acta 52 (2007) 6254.
[24] Z. Liu, B. Guo, S.W. Tay, L. Hong, X. Zhang, J. Power Sources 184 (2008) 16.
[25] S.L. Gojkovic, J. Serb. Chem. Soc. 68 (2003) 859.
[26] S. Papadimitriou, A. Tegou, E. Pavlidou, G. Kokkinidis, S. Sotiropoulos, Electrochim. Acta 52 (2007) 6254.
[27] M.K. Jeon, J.S. Cooper, P.J. McGinn, J. Power Sources 192 (2) (2009) 391.
[28] V. Stamenkovic, T.J. Schmidt, P.N. Ross, N.M. Markovic, J. Phys. Chem. B 106 (2002) 11970.
[29] J.S. Cooper, M.K. Jeon, P.J. McGinn, Electrochem. Commun. 10 (2008) 1545.
[30] M.K. Jeon, Y. Zhang, P.J. McGinn, Electrochim. Acta 54 (2009) 2837.
[31] E. Ding, K.L. More, T. He, J. Power Sources 175 (2008) 794.
[32] M.K. Jeon, P.J. McGinn, J. Power Sources 195 (9) (2010) 2664.
[33] N.D. Morris, T.E. Mallouk, J. Am. Chem. Soc. 124 (2002) 1114.
[34] M.G. Sullivan, H. Utomo, P.J. Fagan, M.D. Ward, Anal. Chem. 71 (1999) 4369.
[35] R. Lin, E.S. Smotkin, J. Electroanal. Chem. 535 (2002) 49.
[36] J.M. Gregoire, M. Kostylev, E.M. Tague, P.F. Mutolo, R.B. van Dover, F.J. DiSalvo, H.D. Abruña, J. Electrochem. Soc. 156 (1) (2009) B160.
[37] J.F. Whitacre, T. Valdez, S.R. Narayanan, J. Electrochem. Soc. 152 (2005) A1780.
[38] R. Jiang, Rev. Sci. Instrum. 78 (2007) 072209.
[39] K. Deshpande, A. Mukasyan, A. Varma, J. Power Sources 158 (2006) 60.
[40] M.K. Jeon, J.H. Liu, K.R. Lee, J.W. Lee, P.J. McGinn, S.I. Woo, Fuel Cells 1 (2001) 133–161.
[41] J.S. Cooper, P.J. McGinn, J. Power Sources 163 (2006) 330.
[42] J.S. Cooper, P.J. McGinn, Appl. Surf. Sci. 254 (2007) 662.
[43] M.K. Jeon, J.S. Cooper, P.J. McGinn, J. Power Sources 185 (2008) 913.
[44] M.K. Jeon, J.S. Cooper, P.J. McGinn, J. Power Sources 188 (2009) 427.
[45] M.K. Jeon, P.J. McGinn, J. Power Sources 194 (2009) 737.
[46] B. Folkesson, R. Larsson, J. Zander, J. Electroanal. Chem. 267 (1–2) (1989) 149.
[47] B. Rajesh, K.R. Thampi, J.M. Bonard, H.J. Mathieu, N. Xanthopoulos, B. Viswanathan, J. Power Sources 141 (2005) 35.
[48] T. Maiyalagan, B. Viswanathan, Mater. Chem. Phys. 121 (1–2) (2008) 165.
[49] K.F. Zhang, D.J. Guo, X. Liu, J. Li, H.L. Li, Z.H. Su, J. Power Sources 162 (2) (2006) 1077.
[50] T. Maiyalagan, F. Nawaz Khan, Catal. Commun. 10 (2009) 433.
[51] C. Roth, N. Benker, R. Theissmann, R.J. Nichols, D.J. Schiffrin, Langmuir 24 (2008) 2191.
[52] X. Zhang, K.Y. Chan, J. Mater. Chem. 12 (2002) 1203.
[53] T. Okada, Y. Suzuki, T. Hirose, T. Ozawa, Electrochim. Acta 49 (2004) 385.
[54] J.H. Zeng, J.Y. Lee, J. Power Sources 140 (2005) 268.
[55] E. Antolini, J.R.C. Salgado, E.R. Gonzalez, J. Power Sources 160 (2006) 957.
[56] A. Bonakdarpour, R. Lobel, R.T. Atanasoski, G.D. Vernstrom, A.K. Schmoeckel, M.K. Debe, J.R. Dahn, J. Electrochem. Soc. 153 (2006) A1835.

[57] H. Yang, N. Alonso-Vante, J.M. Leger, C. Lamy, J. Phys. Chem. B 108 (2004) 1938.
[58] M. Ghanashyam Krishna, Y. Debauge, A.K. Bhattacharya, Thin Solid Films 312 (1998) 116.
[59] C.D. Wagner, W.M. Riggs, L.E. Davis, J.F. Moulder, G.E. Muilenberg, Handbook of X-ray Photoelectron Spectroscopy, Perkin-Elmer, Eden Prairie, MN, 1978.
[60] E. Desimoni, C. Malitesta, P.G. Zambonin, J.C. Riviere, Surf. Interface Anal. 13 (1988) 173.
[61] G.C. Allen, M.T. Curtis, A.J. Hooper, P.M. Tucker, J. Chem. Soc. Dalton Trans. (1973) 1677.
[62] F.H. Stott, Mater. Sci. Technol. 5 (8) (1989) 734.
[63] A. Lippitz, Th. Hübert, Surf. Coat. Technol. 2009 (1–4) (2005) 250.
[64] L.D. Burke, E.J.M. O'Sullivan, J. Electroanal. Chem. 112 (1980) 247.
[65] A. Bonakdarpour, J. Wenzel, J. Electrochem. Soc. 152 (2005) A61.
[66] C.C. Hu, K. Liu, Electrochim. Acta 44 (1999) 2727.
[67] R. Parsons, T. VanderNoot, J. Electroanal. Chem. 257 (1988) 9.